Journal of Atmospheric and Solar-Terrestrial Physics 73 (2011) 1405–1409

Contents lists available at ScienceDirect

Journal of Atmospheric and Solar-Terrestrial Physics

journal homepage: www.elsevier.com/locate/jastp

A computational study of nonresonant cross-field diffusion of energetic particles due to their interaction with interplanetary magnetic decreases

E. Costa Jr.[a,d,*], E. Echer[a], M.V. Alves[a], B.T. Tsurutani[b], F.J.R. Simões Jr.[a], F.R. Cardoso[a], G.S. Lakhina[c]

[a] Instituto Nacional de Pesquisas Espaciais—INPE, P.O. Box 515, 12227-010 S. J. dos Campos, SP, Brazil
[b] Jet Propulsion Laboratory, California Institute of Technology, 4800 Oak Grove Drive, Pasadena, CA 91109, United States
[c] Indian Institute of Geomagnetism, Navi Mumbai, India
[d] Instituto Federal de Minas Gerais – IFMG – Campus Ouro Preto. Rua Pandiá Calógeras, 898, Ouro Preto - MG, 35400-000, Brazil

ARTICLE INFO

Article history:
Received 25 March 2010
Received in revised form
27 January 2011
Accepted 29 January 2011
Available online 5 February 2011

Keywords:
Magnetic decreases
Particles diffusion
Nonresonant interactions
Monte Carlo simulation

ABSTRACT

We present a new method of calculating cross-field diffusion of charged particles due to their interactions with interplanetary magnetic decreases (MDs) in high heliospheric latitudes. We use a geometric model that evaluates perpendicular diffusion to the ambient magnetic field as a function of particle's gyroradius, MD radius, ratio between fields outside and inside the MD, and a random impact parameter. We use Ulysses magnetic field data of 1994 to identify the MDs and get the empirical size and magnetic field decrease distribution functions. We let protons with energies ranging from 100 keV to 2 MeV interact with MDs. The MD characteristics are taken from the observational distribution functions using the Monte Carlo method. Calculations show that the increase in diffusion tends to saturate when particles' gyroradius becomes as large as MD radii, and that particles' gyroradius increases faster than diffusion distance as the energy of the particles is increased.

1. Introduction

Magnetic decreases (MDs) are depressions in the magnitude of the interplanetary magnetic field (IMF) up to 90% of the ambient magnetic field B_0. The decreases were detected in heliospheric latitudes larger than 80° (Tsurutani et al. 1999, 2009; Tsurutani and Ho, 1999; Winterhalter et al., 2000). Magnetic pressure depletions are supplanted by plasma thermal pressure increases. So, MDs are pressure balance structures filled with hot plasma (Winterhalter et al., 1994). Tsurutani et al. (2002b) showed that MHs and MDs are presumably the same phenomenon; however, depending on the region in which they are observed, the mechanism that generates them can be different (Tsurutani et al., 2010).

Protons within these regions are preferentially accelerated perpendicular to the ambient magnetic field (Fränz et al., 2000). Tsurutani et al. (2002b) showed that MDs occur at the phase-steepened edges of Alfvén waves and Tsurutani et al. (2002a) suggested that a diamagnetic effect from the perpendicularly accelerated ions leads to the creation of the MDs. A possible mechanism for the perpendicular ion heating was shown by Dasgupta et al. (2003) to be the ponderomotive force. There are other possible mechanisms, such as beam microinstabilities (Neugebauer et al., 2001), wave–wave interactions (Vasquez and Hollweg, 1999), MHD solitons (Baumgartel, 1999) and the evolution of nonlinear Alfvén waves (Medvedev et al., 1997; Buti et al., 2001).

Charged particle interactions with MDs lead primarily to particle cross-field diffusion due to particle guiding center displacements (Tsurutani and Lakhina, 2004). We use data corresponding to the first time Ulysses passed over the south pole of the heliosphere ($\approx -80^{\circ}$), between August and September of 1994, to investigate such diffusion at high heliospherical latitudes. Tsurutani et al. (1999) obtained observational histograms for MD diameter and magnetic field decrease inside the structures. From these histograms we obtained theoretical curves in which Monte Carlo method was used to select statistical points from the distribution functions of magnetic field decrease and MD spatial size. These MD features and a geometrical model presented by Tsurutani et al. (1999) were used to calculate perpendicular diffusion.

There is a strong interest in particle transport perpendicular to magnetic fields in many kinds of plasmas. Applications include planetary magnetospheres, the interplanetary medium, cosmic ray acceleration and propagation and magnetically confined plasmas. We considered nonresonant diffusion of particles due to interactions with MDs. For the regions of interest these interactions are very effective in causing diffusion. However, other mechanisms can also lead to diffusion, depending on the region and the kind of diffusion under investigation. For cross-field diffusion of cosmic rays, random walk of ambient magnetic field lines have been successfully used (Jokipii, 1966; Jokipii

* Corresponding author. Tel.: +55 31 9197 8712; fax: +55 35 3832 2227.
E-mail address: costajr.e@gmail.com (E. Costa Jr.).

1364-6826/$ - see front matter © 2011 Elsevier Ltd. All rights reserved.
doi:10.1016/j.jastp.2011.01.022

and Parker, 1969; Zimbardo et al., 1995). Verkhoglyadova and le Roux (2005a,b) have considered cross-field diffusion of energetic particles due to the presence of coherent vortex fields. In the field of resonant diffusion, interactions between waves and particles lead mainly to pitch-angle diffusion, and to cross-field diffusion as a second order effect (Landau, 1946; Kennel and Petschek, 1966; Tsurutani and Thorne, 1982; Lyons and Williams, 1984).

This paper is organized as follows. In Section 2 we discuss the data used. Section 3 describes the geometrical model and how the calculations were made. In Section 4 we discuss and interpret the results obtained. Finally, Section 5 gives a discussion and conclusion.

2. Data

Interplanetary magnetic field data used in this work correspond to days 242–268 of 1994 and were first analyzed by Tsurutani et al. (1999). Ulysses distance from the Sun was 2.3 AU and its latitude was -80° over the south pole in this interval. Phillips et al. (1994) demonstrated that the region was filled by a high-speed solar wind ($\approx 750-800$ km s^{-1}) emanating from a polar coronal hole. The time resolution of the data used corresponds to 1 s averages.

Fig. 1 shows a plot of 30 days of IMF data with time resolution of 1 min. The coordinate system is RTN, where $\hat{R}$ points radially outward from the Sun and $\hat{T} = \hat{\Omega} \times \hat{R}/|\hat{\Omega} \times \hat{R}|$, where $\hat{\Omega}$ is the rotation axis of the Sun. The third vector, $\hat{N}$, completes the right-hand system. The top panel corresponds to B_R, second panel is B_T, third one is B_N and bottom panel corresponds to total field magnitude B. It is possible to see a lot of depletion periods in the magnitude of the field, indicating the presence of MDs.

Tsurutani et al. (1999) identified 129 MDs between days 242 and 268 of 1994 and the distributions of MDs features were presented. After forming histograms of the data, histograms were fitted for MDs sizes and field decreases, respectively:

$$y = 38.5e^{-1.5\times10^{-5}dm} \quad (1)$$

and

$$y = 5.4 + 348.7e^{-8\Delta B}, \quad (2)$$

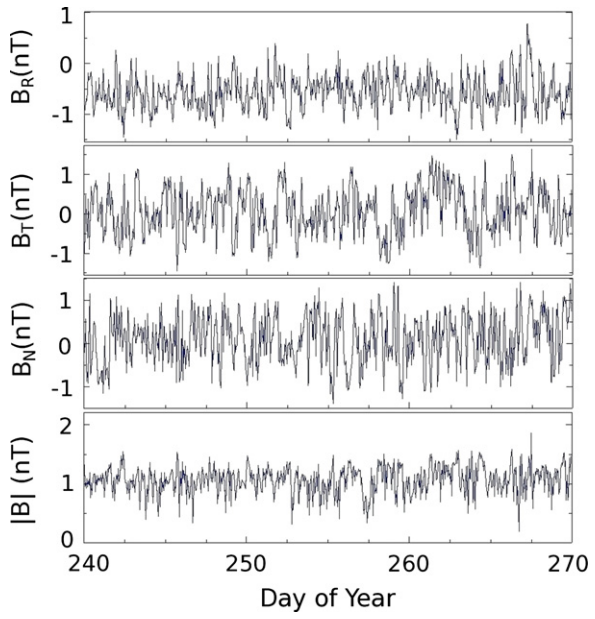

Fig. 1. Interplanetary Ulysses magnetic field data between days 240 and 270 of 1994 at high heliographic latitudes. From the top: B_R, B_T, B_N and magnitude of B.

where dm is the MD diameter in kilometers, ΔB is the ratio between magnetic field inside (B_{MD}) and outside (B_0) the structure (B_{MD}/B_0) and y is the observational percentage of events. MDs diameters were obtained by multiplying their temporal duration by solar wind speed. The Monte Carlo method was used to get representative points from Eqs. (1) and (2) to make the calculations.

3. Geometrical model and method of calculation

The geometrical model used in this work is based on an idealized and mathematically treatable case. We will show that significant results can be obtained from it. Fig. 2 shows the basic geometry of the interaction between a charged particle and a MD. Initially, the particle moves around its guiding center in a uniform magnetostatic field B_0 (directed into the paper), with gyroradius r. As a simplification, here we assume that the MDs have a circular cross-section of radius a and a cylindrical structure in a 3D view aligned along the magnetic field. The distance from the guiding center of the particle to the center of the MD is d, the impact parameter of the interaction. We also consider that within the MD the field (B_{MD}) is in the same direction as the ambient magnetic field. The MD radii "a" considered in this paper are in the range from 1.25×10^3 to 2×10^5 km, while the Larmour radii "r" of the particles used are in the interval from 3.23×10^4 to 1.45×10^5 km. The MD radius is, to first order, independent of the magnitude of the decrease. They are independent parameters and it makes the modeling of particle interaction with MDs simpler (Tsurutani et al., 1999).

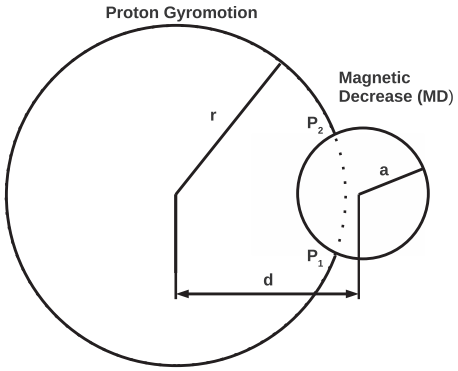

Fig. 2. Geometry of the interaction of a charged particle of gyroradius r and a MD of radius a (Tsurutani et al., 1999).

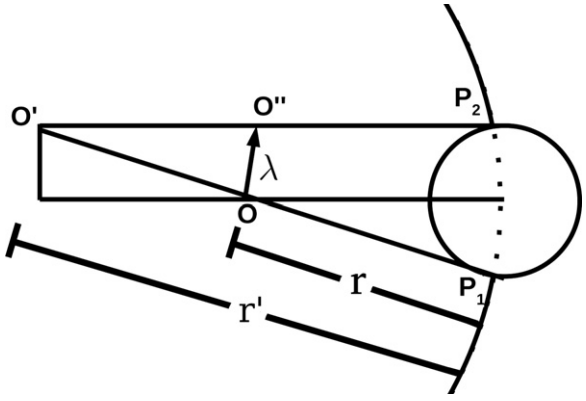

Fig. 3. Illustration showing cross-field displacement of the guiding center of a charged particle after interacting with a MD (Tsurutani et al., 1999).

Fig. 3 illustrates how the particle guiding center will be displaced perpendicularly to the magnetic field due to the interaction between the particle and the MD. Initially the guiding center is at point O. The interaction takes place at point P_1. Due to a huge gradient in the magnetic field strength from B_0 to B_{MD}, particle's first adiabatic invariant is broken and the gyrocenter becomes point O'. Inside the MD the gyroradius r' is given by $r(B_0/B_{MD})$. When the particle leaves the MD at point P_2 the new gyrocenter is located at point O''. The net result of such interaction is that the particle's gyrocenter has moved from point O to point O'', a distance λ apart from each other.

It is possible to determine geometrically the expression for the displacement of the particles's guiding center perpendicular to B_0. Further figures and geometrical calculations are needed, but are not shown here (for more details see Tsurutani et al., 1999; Tsurutani and Lakhina, 2004). The expression for λ as a function of the magnetic field inside and outside the MD and the geometrical parameters shown in Fig. 2 is given by

$$\lambda = \frac{2(m-1)}{m}\sqrt{a^2 - \frac{\left(a^2+d^2+r^2(1-2m)+d(m-1)\sqrt{\frac{(-a^2+d^2+r^2)^2}{d^2}}\right)^2}{4\left(d^2+r^2(m-1)^2+d(m-1)\sqrt{\frac{(-a^2+d^2+r^2)^2}{d^2}}\right)}}, \quad (3)$$

where m is the ratio between B_0 and B_{MD} ($m = B_0/B_{MD}$).

In order to calculate a particle's guiding center displacement for interactions with "n" number of MDs it is necessary to solve Eq. (3) "n" times and account the displacement for the several interactions. In present calculations we investigated interactions with 100 and 200 MDs (n=100 and 200, respectively). The ambient field B_0 was set as constant, $B_0 = 1.2$ nT. The gyroradius r is also constant, depending only on particle's energy. Statistically, the MD radius a (one-half of dm) was taken from Eq. (1) and m (ΔB^{-1}) came from Eq. (2). The impact parameter d is randomly selected in the range where the interaction can take place ($|r-a| < d < |r+a|$). Besides this, interactions can occur at any angle θ of particle's trajectory, as they really occur in space ($0 \le \theta \le 2\pi$).

We used the Monte Carlo method to sample as accurately as possible the properties of Eqs. (1) and (2), getting the values of the variables a and m, respectively. The MCM consists in starting with a random initial value for a variable (we call it initial state i). After this, a possible new value is selected for the variable (we call it the new state j) with a selection probability T_{ij}. The new state can be accepted with probability P_{ij}^{acc}, with the system moving from state i to j, or it is rejected with probability $1-P_{ij}^{acc}$, with the system staying at the same state as it was before. Each state accepted by the method becomes state i and a possible new state is selected. The process is repeated until a sufficient number of states is selected. The set of all selected values for a variable is used in the calculations, in which each pair of values a and m represents a different MD. The sequence of states generated by the MCM is called a Markov Chain, because the transition probability only depends on the present state but not on the previous (Amar, 2006; Binder, 1996).

The simplest and more commonly used equation for the acceptance probability P_{ij}^{acc} corresponds to the Metropolis–Hastings rule (Amar, 2006):

$$P_{ij}^{acc} = \min\left(1, \frac{P_j T_{ji}}{P_i T_{ij}}\right), \quad (4)$$

where P_i and P_j correspond to the values of the function as calculated for the states i and j, respectively, obtained by Eqs. (1) and (2).

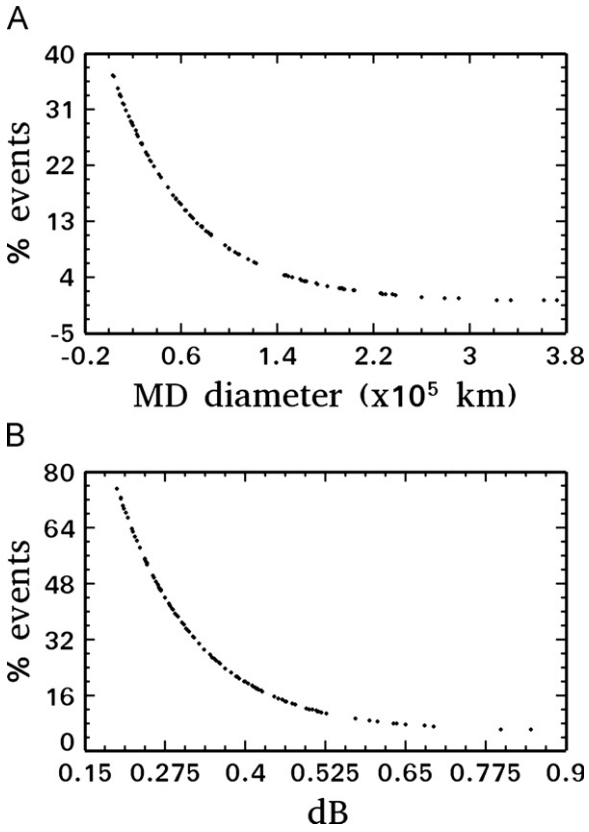

Fig. 4. Example of discrete curves obtained by Monte Carlo method. Panel (A) corresponds to MD diameter in kilometers and panel (B) corresponds to ΔB.

4. Results and discussion

Fig. 4 shows examples of discrete curves corresponding to Eqs. (1) and (2), respectively. Each curve contains 100 points representing 100 different MDs. The points were obtained by the Monte Carlo method. For the MCM we used symmetric selection rates as a simplification, what is $T_{ij} = T_{ji}$ in Eq. (4). It means that from a present state i, the probability of selecting a possible new state j is the same that from a state j selecting a possible new state i for a given variable. Eq. (4) becomes much simpler with this assumption, $P_{ij}^{acc} = \min(1, P_j/P_i)$.

We have made the calculation of cross-field diffusion for protons of 20 different energies ranging from 100 keV to 2 MeV, separated by intervals of 100 keV. Particle pitch angles are assumed to be 45°, which means that half of the particle's kinetic energy is perpendicular to the magnetic field ($E_\perp$) and half is in the parallel direction ($E_\parallel$). First, we let 1000 particles of each energy interact with 100 different MDs (n=100) at different points of their trajectories and with random impact parameters. In order to investigate how the number of MDs changes the diffusion distance, we also did the calculations using 200 MDs (n= 200).

One important result is that when the perpendicular energy of a particle is increased, the corresponding increase in its gyroradius is larger than the increase in diffusion distance. Fig. 5 shows the results of perpendicular displacements normalized by gyroradius for the case of 200 MDs. While diffusion for protons of perpendicular energy of 100 keV goes up to 60 gyroradii, for protons with perpendicular energy of 1 MeV it goes only to 25 gyroradii. Most of the particles are displaced between 10% and 50% of the maximum displacement. Although we show only the results corresponding to four different energies in this paper, results corresponding to other energies and to the interaction

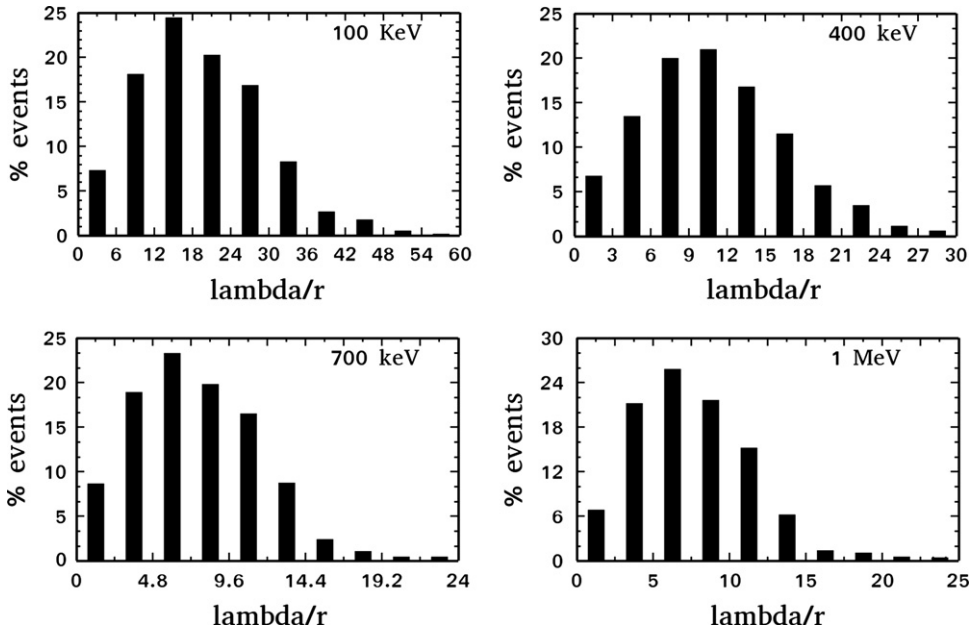

Fig. 5. Diffusion distance normalized by gyroradius for the case of 200 MDs and perpendicular energies of 100, 400, 700 keV and 1 MeV.

with 100 MDs are qualitatively the same. Peaks of occurrence lies between 20% and 40% of the maximum displacement.

As our model of interaction between particles and MDs is based on random parameters, such as the impact parameter and the point of interaction, a lot of variations are expected for a given case. To avoid this, in order to obtain the perpendicular diffusion distance, we run the model 10 times for each energy to get an average value. Each time we run it to generate a different set of MDs and calculate the displacement λ_k ($k=1$ to 10) for the 1000 particles. After doing that 10 times, we calculate the average diffusion distance $\langle \lambda_k \rangle$ for a specific energy. Fig. 6 shows how large these fluctuations can be at each energy. Blue circles represent each one of the 10 λ_k and red squares represent the average diffusion distance.

In order to compare how the diffusion varies in the two cases (interaction of each particle with 100 and 200 MDs) we define an average rate of growth based on a linear fit for the values of average diffusion (red squares shown in Fig. 6). We made fits of the type $y=\alpha x+\beta$, where the value of α tells us how the diffusion grows with increasing perpendicular energy. The range where the fit is applied is 50 keV $\leq E_\perp \leq$ 400 keV. For perpendicular energies higher than 400 keV the diffusion presents a tendency to saturation and the increase of λ with increasing perpendicular energy is much smaller. It happens because the Larmour radii r of the particles become as large as MDs radii a. For the case of 100 MDs $\alpha=450.8$ and for the case of 200 MDs $\alpha=608.9$, which means that diffusion increases on average 450.8 and 608.9 m by each increase of 1 eV in protons perpendicular energy, respectively.

Although the number of MDs was doubled from 100 to 200, diffusion did not increase proportionally. The corresponding increase in diffusion after doubling the number of MDs is about 35%. It would not be expected that doubling the number of MDs would lead to a diffusion twice as large, once the interactions take place in an isotropic space perpendicularly to the magnetic field.

It is important to notice that the diffusion caused by such interactions is considerable. For the case of 100 MDs perpendicular diffusion goes from 4.37×10^8 to 6.84×10^8 m and for 200 MDs it goes from 6.30×10^8 to 9.40×10^8 m. The case of maximum diffusion corresponds to $\approx$0.63% of one astronomical unit or $\approx$147 Earth Radii.

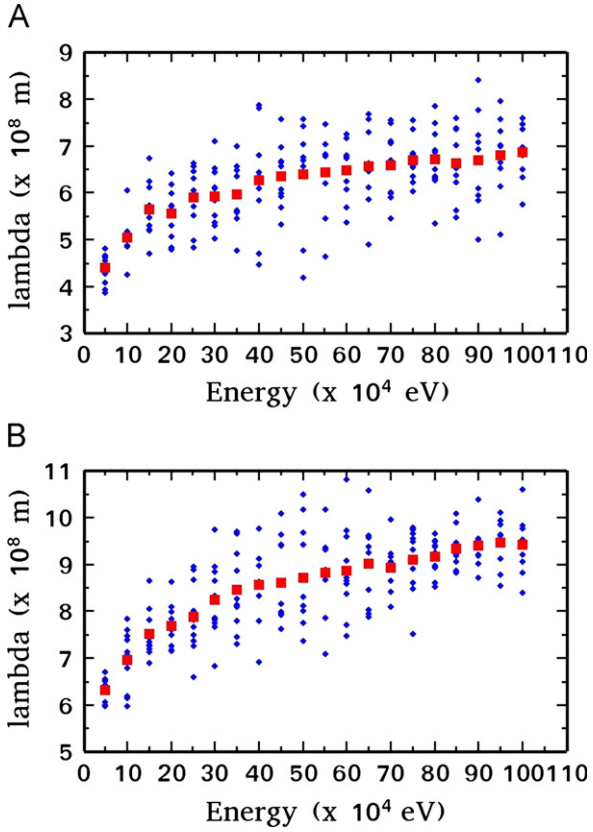

Fig. 6. Values of λ in function of perpendicular energies. Blue circles represent λ and red squares represent the average of the 10 values of λ to each energy. Panel (A) corresponds to interaction with 100 MDs and panel (B) corresponds to 200 MDs. (For interpretation of the references to color in this figure legend, the reader is referred to the web version of this article.)

In order to compare diffusion in different regions in future works, we define a diffusion coefficient as $D_\perp=\langle\lambda^2\rangle/\Delta t$, where Δt is the time one particle takes to go from one MD and the next one. Notice that it depends on the distance between the MDs, given by the data, and the energy of the particles. Here, from the

data, we consider an average distance between the MDs to obtain Δt. For the present case $\Delta t \approx 4520$ and 1000 s for particles of parallel energy of 50 keV and 1 MeV, which means that particles with these parallel energies hits an MD each 4520 and 1000 s, respectively. As parallel speed of particles considered are much higher than solar wind speed, the speed the MDs are convected, solar wind speed are not taken into account in the calculations of Δt. For energies considered, the diffusion coefficient ranges in the interval $5.42 \times 10^{11}\ \mathrm{m^2\ s^{-1}} \leq D_{\perp} \leq 5.95 \times 10^{12}\ \mathrm{m^2\ s^{-1}}$.

5. Discussion

Monte Carlo simulations were made for perpendicular diffusion in high heliospheric latitudes. Interactions between charged particles and MDs in high heliospheric latitudes can lead to large cross-field diffusion in particle guiding centers as high as $\approx 0.63\%$ AU for the case of particles of 2 MeV energy interacting with 200 MDs.

One important result is that diffusion distance increases slower than gyroradius with increasing energy, as can be seen from Fig. 5. This fact leads to a tendency of saturation in diffusion for perpendicular energies above 400 keV, where particles' gyroradius becomes as large as MDs radii or larger. For perpendicular energies higher than 400 keV the effect of the interactions is physically smaller.

The method presented here was made mathematically tractable by using approximations that simplified the calculations. Results obtained are physically consistent. The method can be employed to calculate cross-field diffusion of heavy ions and electrons, and for other space environment regions such as interplanetary space at low latitudes, planetary magnetosheaths, interplanetary shocks, heliospheric sheaths and astrophysical plasmas. However, it is necessary to take into account the particularities of the MDs in the regions under investigation.

Future works should include calculations of perpendicular diffusion in near ecliptic plane regions, where MDs are more frequent. By making calculations in low heliospheric latitudes, it will be possible to study the differences in MDs and diffusion features in high and low latitudes.

Acknowledgments

The authors would like to thank Brazilian agencies: Conselho Nacional de Desenvolvimento Científico e Tecnológico (CNPq - project 140441/2006-9), Coordenação de Aperfeiçoamento de Pessoal de Nível Superior (CAPES) and Fundação de Amparo à Pesquisa do Estado de São Paulo (FAPESP - project 2008/01288-0) for financial support. G.S.L. thanks the Indian National Science Academy, New Delhi, for the support under the Senior Scientist Scheme.

References

Amar, J.G., 2006. The Monte Carlo method in science and engineering. Computing in Science and Engineering 8, 9–19.

Baumgartel, K., 1999. Soliton approach to magnetic holes. Journal of Geophysical Research 104, 28295–28308.

Binder, K., 1996. Monte Carlo Methods in Statistical Physics. Springer-Verlag, Germany.

Buti, B., Tsurutani, B.T., Neugebauer, M., Goldstein, B.E., 2001. Generation mechanism for magnetic holes in the solar wind. Geophysical Research Letters 28, 1355–1358.

Dasgupta, B., Tsurutani, B.T., Janaki, M.S., 2003. A kinetic approach to the ponderomotive force. Geophysical Research Letters 30, 11,1–11,4.

Fränz, M., Borgess, D., Horbury, T.S., 2000. Magnetic field depressions in the solar wind. Journal of Geophysical Research 105, 12,725–12,732.

Jokipii, J.R., 1966. Cosmic-ray propagation. I. Charged particles in a random magnetic field. The Astrophysical Journal 146, 480.

Jokipii, J.R., Parker, E.N., 1969. Stochastic aspects of magnetic lines of force with application to cosmic-ray propagation. The Astrophysical Journal 155, 777.

Kennel, C.F., Petschek, H.E., 1966. Limit on stably trapped particle fluxes. Journal of Geophysical Research 71, 1.

Landau, L.P., 1946. On the vibrations of the electronic plasma. Journal of Physics Moscow, 25.

Lyons, L.R., Williams, D.J., 1984. Quantitative Aspects of Magnetospheric Physics. Reidel, Boston.

Medvedev, M.V., Schevchenkp, V.I., Diamond, P.H., Galinsky, V.L., 1997. Fluid model for kinetic effects on coherent nonlinear Alfvén waves: numerical solutions. Physics of Plasmas 4, 1257–1285.

Neugebauer, M., Goldstein, B.E., Winterhalter, D., Smith, E.J., Gary, S.P., MacDoWall, R.J., 2001. Ion distribution in large magnetic holes in the fast solar wind. Journal of Geophysical Research 106, 5635–5648.

Phillips, J.L., Balogh, A., Bame, S.J., Goldstein, B.E., Gosling, J.T., Hocksema, J.T., McComas, D.J., Neugebauer, M., Sheeley, N.R., Wang, Y.M., 1994. Ulysses at 50° south: constant immersion in the high speed solar wind. Geophysical Research Letters 21, 1105–1108.

Tsurutani, B.T., Dasgupta, B., Galvan, C., Neugebauer, M., Lakhina, G.S., Arballo, J.K., Winterhalter, D., Goldstein, B.E., Buti, B., 2002a. Phase-steepened Alfvèn waves, proton perpendicular energization and creation of magnetic holes and magnetic decreases: the ponderomotive force. Geophysical Research Letters 29, 23,1–23,4.

Tsurutani, B.T., Galvan, C., Arballo, J.K., Winterhalter, D., Sakurai, R., Smith, E.J., Buti, B., Lakhina, G.S., Balogh, A., 2002b. Relationship between discontinuities, magnetic holes, magnetic decreases, and nonlinear Alfvén waves: Ulysses observations over the solar poles. Geophysical Research Letters 29, 23,1–23,4.

Tsurutani, B.T., Guarnieri, F.L., Echer, E., Lakhina, G.S., Verkhoglyadova, O.P., 2009. Magnetic decrease formation from <1 to ≈ 5 AU: CIR reverse shocks. Journal of Geophysical Research 114, 1–14.

Tsurutani, B.T., Ho, C.M., 1999. A review of discontinuities and Alfvén waves in interplanetary space: Ulysses results. Reviews of Geophysics 37, 517–542.

Tsurutani, B.T., Lakhina, G.S., 2004. Cross-field particle diffusion in a collisionless plasma: a nonresonant and a resonant mechanism. In: CP 703, Plasmas in the Laboratory and in the Universe. AIP Publications, New York.

Tsurutani, B.T., Lakhina, G.S., Verkhoglyadova, O.P., Echer, E., Guarnieri, F.L., 2010. Magnetic decreases (MDs) and mirror mode: two different plasma β changing mechanisms. Nonlinear Processes in Geophysics 17, 1–13.

Tsurutani, B.T., Lakhina, G.S., Winterhalter, D., Arballo, J.K., Galvan, C., Sakurai, R., 1999. Energetic particle cross-field diffusion: interaction with magnetic decreases (MDs). Nonlinear Processes in Geophysics 6, 235–242.

Tsurutani, B.T., Thorne, R.M., 1982. Diffusion processes in the magnetopause boundary layer. Geophysical Research Letters 9, 1247–1250.

Vasquez, B.J., Hollweg, J.V., 1999. Formation of pressure balance structures and fast waves from nonlinear Alfven waves. Journal of Geophysical Research 104, 4681–4696.

Verkhoglyadova, O.P., le Roux, J.A., 2005a. Anomalous and classical diffusion of cosmic rays due to nonlinear two-dimensional structures and random magnetic fields. Journal of Geophysical Research 110, A10S03.

Verkhoglyadova, O.P., le Roux, J.A., 2005b. Particle transport in a vortex medium. Advances in Space Research 35, 660–664.

Winterhalter, D., Neugebauer, M., Goldstein, B.E., Smith, E.J., Bame, S.J., Balogh, A., 1994. Ulysses field and plasma observations of magnetic holes in the solar wind and their relation to mirror-mode structures. Journal of Geophysical Research 99, 23,371–23,381.

Winterhalter, D.E., Smith, E.J., Neugebauer, M., Goldstein, B.E., Tsurutani, B.T., 2000. The latitudinal distribution of solar wind magnetic holes. Geophysical Research Letters 27, 1615–1618.

Zimbardo, G., Veltri, P., Principato, S., 1995. Anomalous diffusion and levy random walk of magnetic field lines in three dimensional turbulance. Physical Review E 61, 1940.